1552 Induction Hardened Steel Iteration #92

Fatigue Behavior, Monotonic Properties and Microstructural Data

Prepared by:

A.A. Rteil
and
T.H. Topper

Department of Civil Engineering
University of Waterloo
Waterloo, Ontario Canada

Prepared for:
The AISI Bar Steel Applications Group

November 2006

American Iron and Steel Institute
2000 Town Center, Suite 320
Southfield, Michigan 48075
tel: 248-945-4777
fax: 248-352-1740
www.autosteel.org

TABLE OF CONTENTS

SUMMARY

This report presents the monotonic and fatigue test results obtained for 1552 Induction Hardened (simulated case) (It 92) steel. The material was provided by the American Iron and Steel Institute (AISI). Monotonic tensile tests were performed to measure the yield strength, the tensile strength and the reduction of area. Strain-controlled constant-amplitude fatigue tests were to obtain the strain-life curve, cyclic stress-strain curve and fatigue data for this material. Also the microstructure data was obtained.

INTRODUCTION

This report presents the results of tensile and fatigue tests performed on group of 1552 Induction Hardened-simulated case (It 92) steel samples. The material was provided by the American Iron and Steel Institute. The objectives of this investigation were to obtain the microstructure data, mechanical properties, cyclic stress-strain data and strain-life fatigue data requested by the AISI bar group.

EXPERIMENTAL PROCEDURE

Specimen Preparation

The material for the study was received in the form of 1.01" round bars. Smooth cylindrical fatigue specimens, shown in Figure 1, were machined from the cylindrical bars and induction hardened. Then, the gauge sections of the fatigue specimens were mechanically polished in the loading direction. Before testing, the specimens had a final polish in the loading direction in the gauge sections using 600-emery paper and a thin band of M-coat D acrylic coating was applied along the central gauge section. The purpose of the M-coat D application was to prevent scratching of the smooth surface by the knife-edges of the strain extensometer, thus reducing the incidence of knife-edge failures.

Test Equipment and Procedure

Monotonic tension tests were performed to determine the yield strength, the tensile strength, the percent elongation and the percent reduction of area. Hardness tests were performed on the surface of three fatigue specimens using a Rockwell C scale. The hardness measurements were repeated three times for each specimen and the average value was recorded.

All fatigue tests were carried out in a laboratory environment at approximately 25^{o}C using an MTS servo-controlled closed loop electro-hydraulic testing machine. A process control computer, controlled by FLEX software [1] was used to output constant strain and stress amplitudes in the form of a sinusoidal wave.

Axial, constant amplitude, fully reversed (R=-1) strain-controlled fatigue tests were performed on smooth specimens. The stress-strain limits for a given cycle of each specimen were recorded at logarithmic intervals throughout the test via a peak reading voltmeter. Failure of a specimen was defined as a 50 percent drop in tensile peak load from the peak load observed at one half the

expected specimen life. For fatigue lives greater than 100,000 reversals, the specimens were tested in stress-control once the stress-strain loops had stabilized. For the stress-controlled tests, failure was defined as the separation of the smooth specimen into two pieces. For strain-controlled tests the loading frequency varied from 0.03 Hz to 3 Hz while in stress-controlled tests the frequency used was up to 75 Hz.

RESULTS

Chemical composition and microstructure Data

The chemical composition as provided by the supplier is shown in Table 1. Figure 2 presents the martensite microstructure of the 1552 Ind. Hard. steel. Figure 3 shows the inclusions observed in this material.

Strain-Life Data

Constant amplitude test data obtained in this investigation are given in table 2. The stress amplitude corresponding to the strain amplitude was calculated from the peak load amplitude at the specimen half-life.

A fatigue strain life curve is shown in Figure 4, and is described by the following equation:

$$\frac{\Delta\varepsilon}{2} = \frac{\sigma'_f}{E}(2N_f)^b + \varepsilon'_f(2N_f)^c \qquad \text{Eq 1}$$

where $\frac{\Delta\varepsilon}{2}$ = True total strain amplitude

$2N_f$ = Number of reversals to failure

σ'_f = Fatigue strength coefficient

b = Fatigue strength exponent

ε'_f = Fatigue ductility coefficient

c = Fatigue ductility exponent

The values of the strain-life parameters were determined from the best fit curve of the fatigue testing data and presented in table 3.

Cyclic Stress-Strain Curves

Stabilized, half-life stress data obtained from strain-life fatigue tests were used to obtain the companion cyclic stress-strain curve shown in Figure 5. The cyclic stress-strain curve is described by the following equation:

$$\varepsilon = \frac{\sigma}{E_c} \qquad \text{Eq 2}$$

where ε = True total strain amplitude

σ = cyclically stable true stress amplitude

E_c = Cyclic modulus of elasticity

The constant E_c obtained from a best fit of the above equation to the test data are given in table 3.

Mechanical Properties

The engineering monotonic tensile stress-strain curves are given in Figure 6. The true monotonic and true cyclic stress-strain curves plotted together are given in Figure 7. The monotonic properties along with the average hardness test results are included in table 3. The individual hardness measurements are given in Table 2.

OBSERVATIONS

This material (It 92) exhibited a low fatigue strength (Fig. 4) as well as a low monotonic strength (Fig. 6). A fractographic SEM analysis was completed at DaimlerChrysler on a fatigue specimen that failed during initial loading. The metallographic results are included with this report (Appendix 1). The results of the SEM analysis showed that failure initiated by an intergranular mode and exhibited increasing amounts of microvoid coalescence as the fracture propagated. A similar analysis on a fatigued specimen is to be presented at the next AISI Bar Fatigue Committee Meeting (scheduled Dec. 7, 2006).

REFERENCES

[1] Pompetzki, M.A., Saper, R.A., and Topper, T.H., "Software for High Frequency Control of Variable Amplitude Fatigue Tests," Canadian Metallurgical Quarterly, Vol. 25, No. 2, pp. 181-194, 198.

[2] J. A. Bannantine, J. J. Comer, and J. L. Handrock (1990), In :Fundamentals of Metal Fatigue Analysis, Prentice Hall, London.

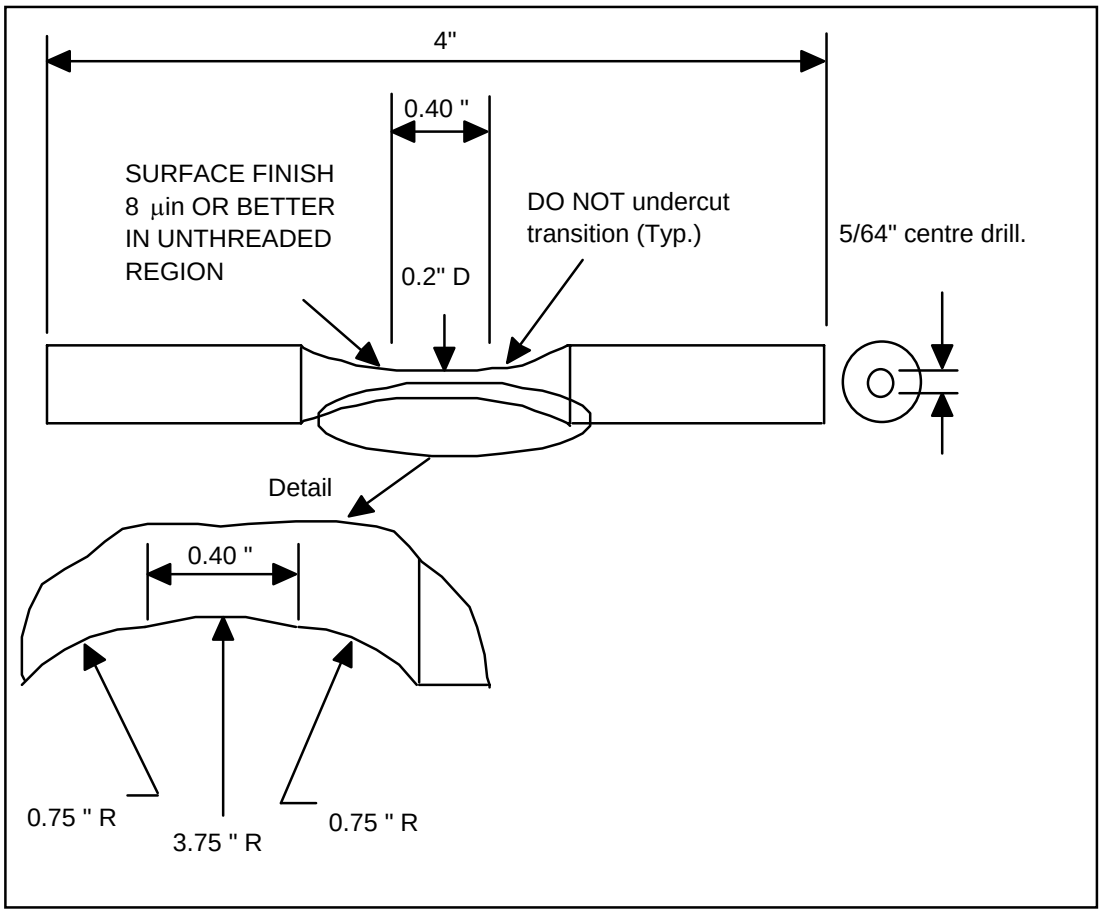

Figure 1 Smooth cylindrical fatigue specimen

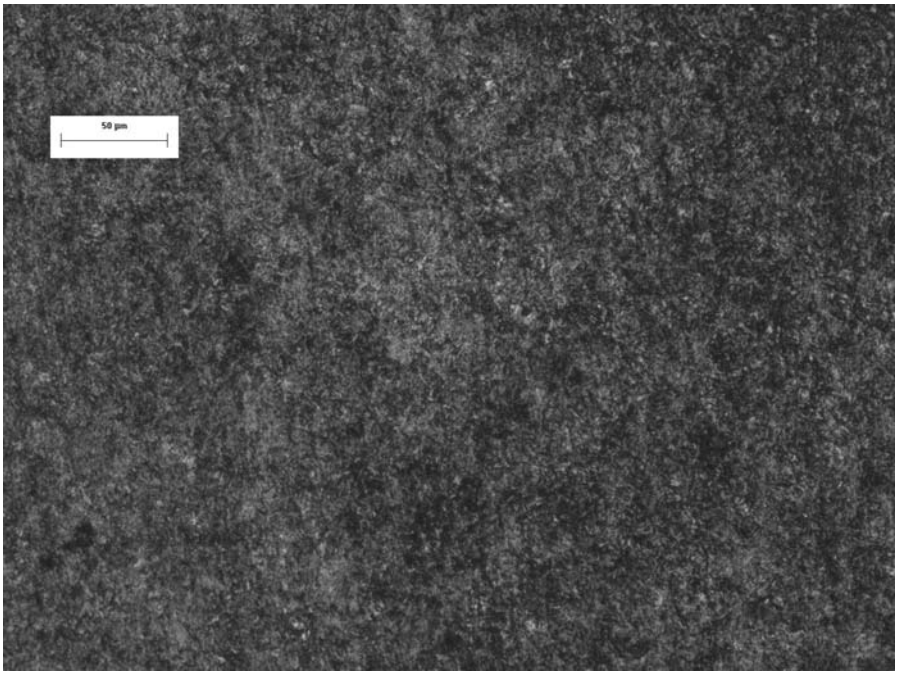

Figure 2 Photomicrographs of 1552 Induction Hardened (It 92) steel.

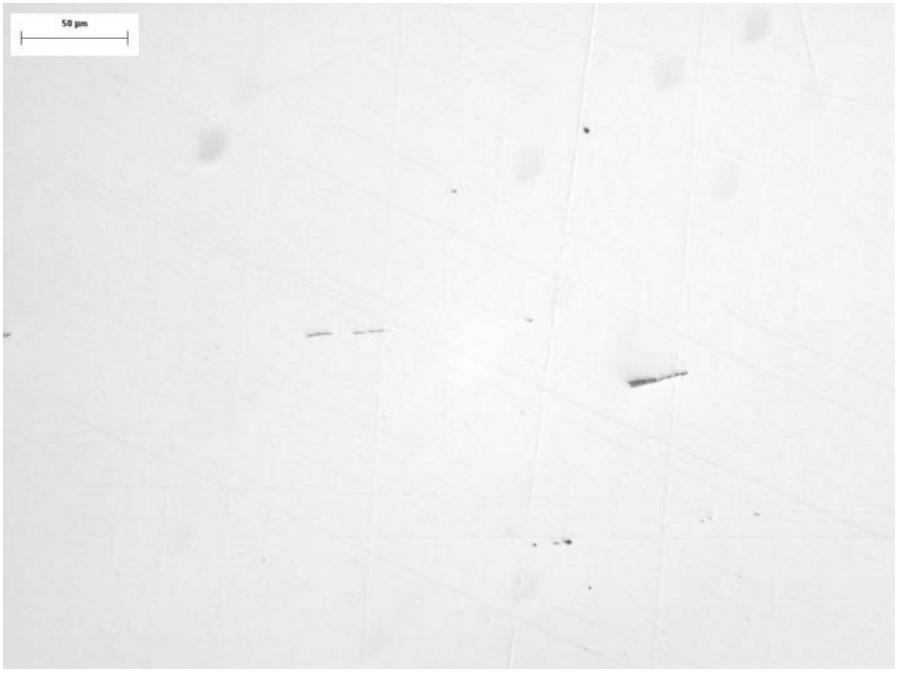

Figure 3 Inclusions 1552 Induction Hardened (It 92) steel.

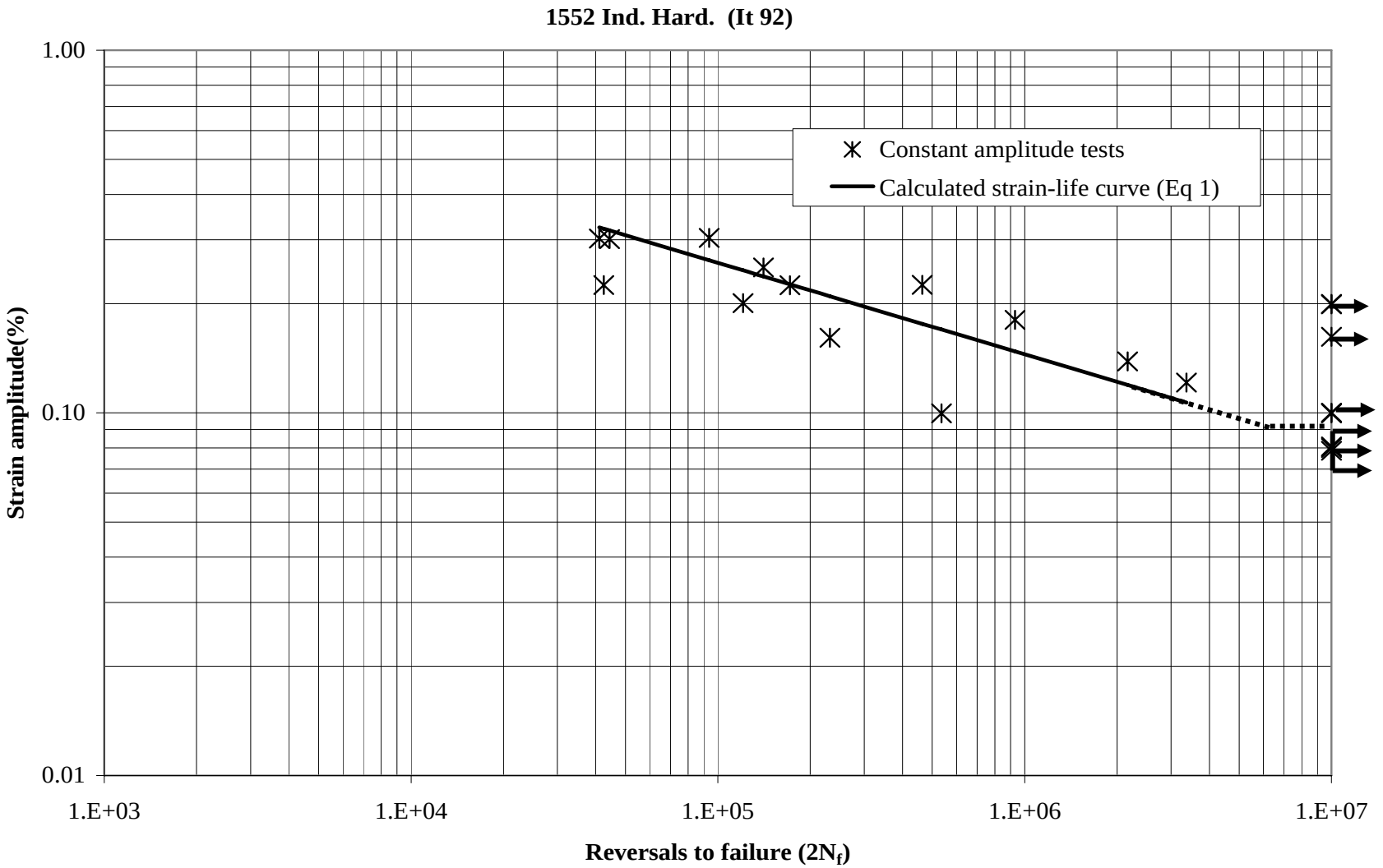

Figure 4. Constant amplitude fully reversed strain-life curve for Iteration 92

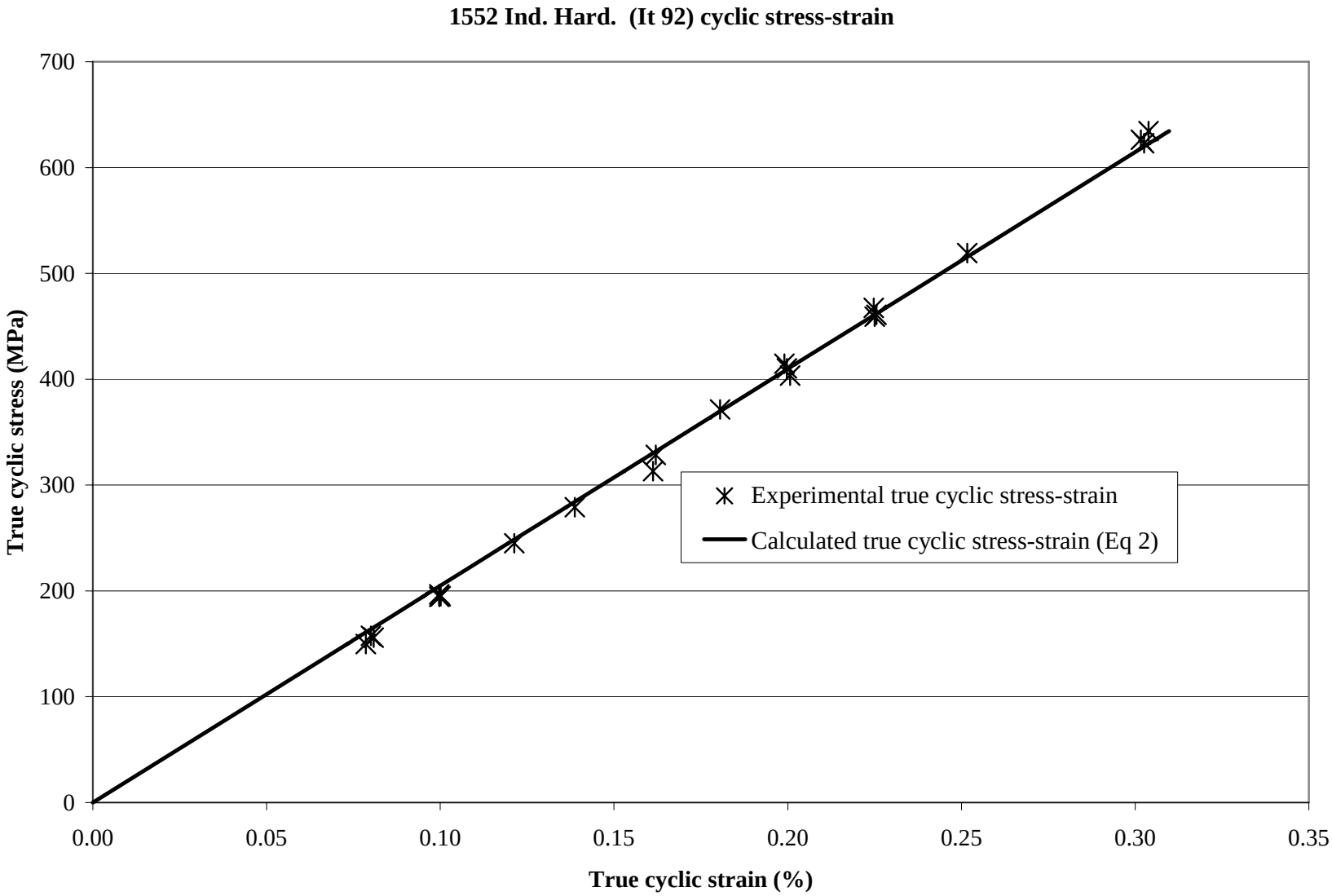

Figure 5. Cyclic true stress-strain curve for iteration 92

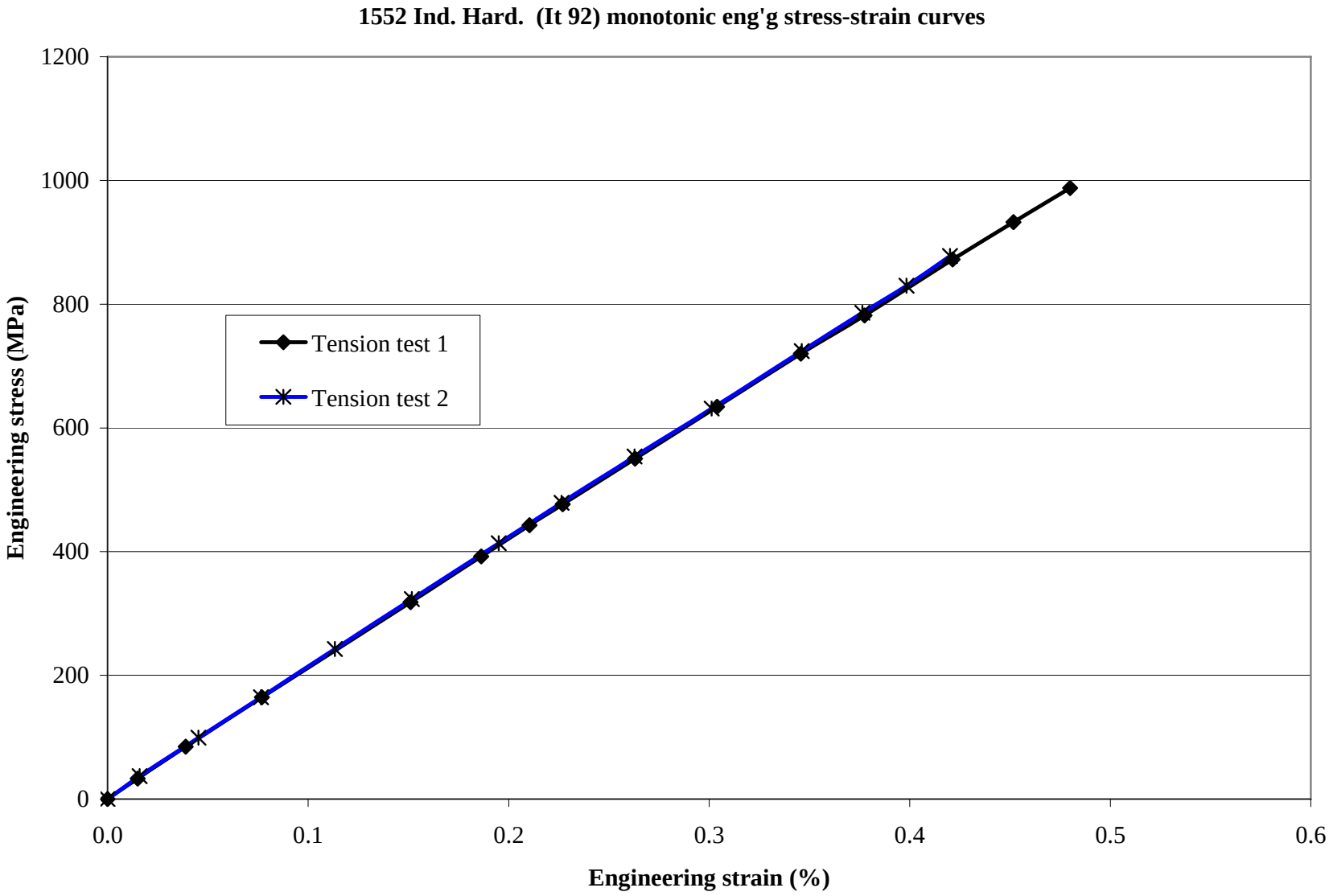

Figure 6. Tensile monotonic engineering stress-strain curves for iteration 92

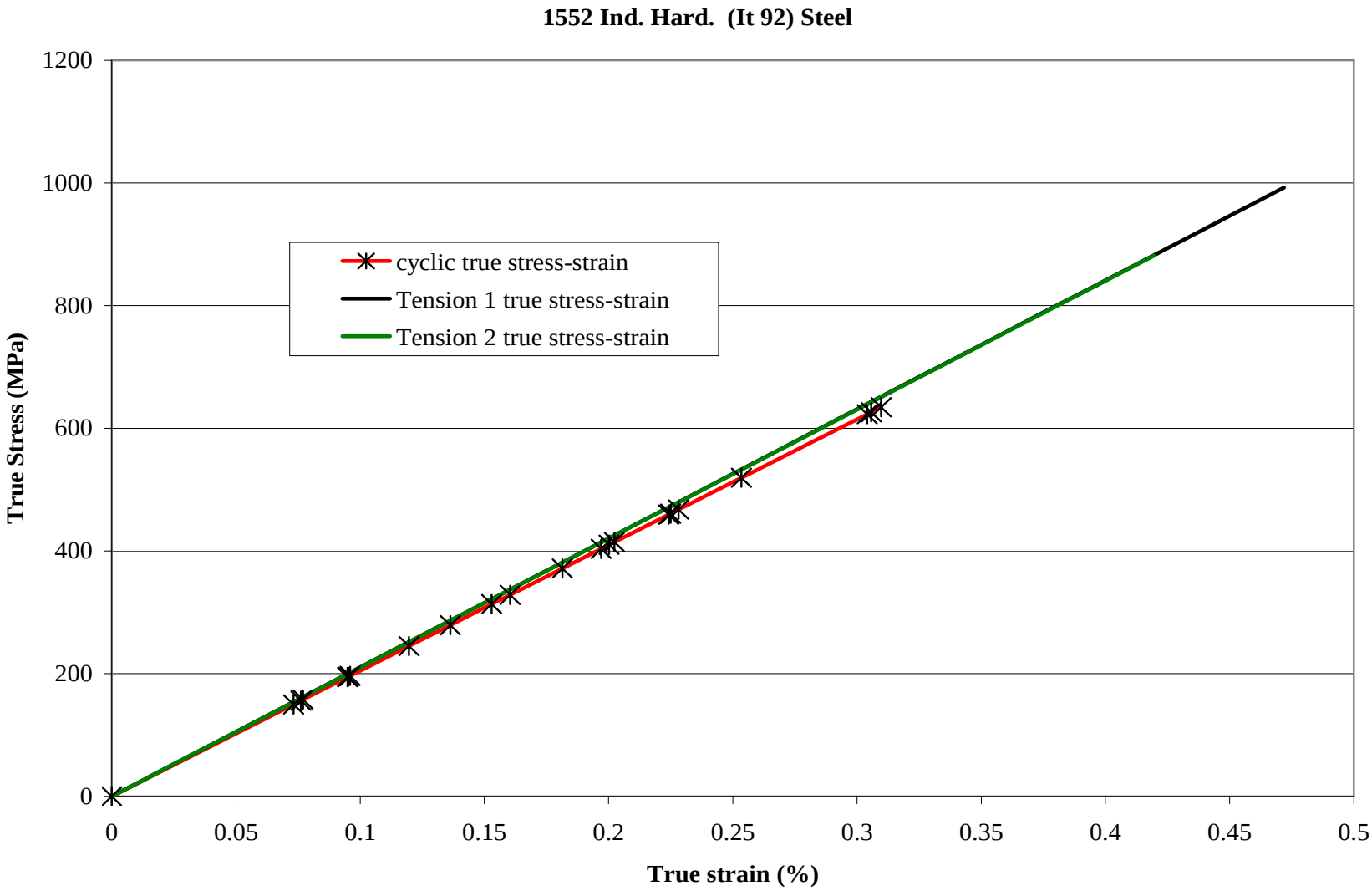

Figure 7. Monotonic and Cyclic true stress-strain curves for iteration 92

Table 1: Chemical composition for Iteration 92

Chemical element	Quantity (%)
Carbon—C	0.52
Manganese (Mn)	1.43
Phosphorus (P)	0.011
Sulfur (S)	0.012
Silicon (Si)	0.24
Copper (Cu)	0.09
Nickel (Ni)	0.09
Chromium (Cr)	0.1
Molybdenum (Mo)	0.01
Tin (Sn)	0.005
Aluminum (Al)	0.001
Vanadium (V)	0.066
Columbium(Cb) /Niobium (Nb)	0.001
Titanium (Ti)	0.001
Boron (B)	0.0003
Calcium (Ca)	0
Zirconium (Zr)	0.001
Nitrogen (ppm) (N)	0.0115
Oxygen (ppm) (O)	0
Co	0.005
Zn	0.0019
Pb	0.0001
ASA	0.000

Table 2: Fatigue Data for Iteration 92

Sp#	Total Strain Amplitude (%)	Stress Amplitude (MPa)	Plastic Strain Amplitude (%)	Elastic Strain Amplitude (%)	(50% load drop) Fatigue Life (Reversals, 2Nf)	Hardness (Rockwell C)
3	0.304	634.5	0.00	0.304	93,590	
4	0.252	519.2	0.00	0.252	140,938	
5	0.225	459.2	0.00	0.225	42,500	
6	0.225	460.8	0.00	0.225	463,802	
23	0.225	467.4	0.00	0.225	171,904	57
7	0.201	403.5	0.00	0.201	120,832	
20	0.200	410.1	0.00	0.200	10,000,000*	
22	0.199	414.5	0.00	0.199	10,000,000*	
8	0.181	371.6	0.00	0.181	930,010	57
9	0.161	313.2	0.00	0.161	231,954	
18	0.162	328.6	0.00	0.162	10,000,000*	
10	0.139	279.1	0.00	0.139	2,164,318	
11	0.121	245.0	0.00	0.121	3,371,464	57
12	0.100	196.6	0.00	0.100	10,000,000*	
14	0.100	195.0	0.00	0.100	10,000,000*	
16	0.100	194.4	0.00	0.100	535,474	
17	0.081	155.9	0.00	0.081	10,000,000*	
19	0.079	149.9	0.00	0.079	10,000,000*	
21	0.080	157.6	0.00	0.080	10,000,000*	

* Run out

Table 3: Monotonic and cyclic properties for iteration 92

Monotonic Properties	
Average Elastic Modulus, E (GPa)	210.2
Yield Strength (MPa)	N/A
Ultimate tensile Strength (MPa)	933
% Elongation (%)	0.5
% Reduction of Area (%)	0.0
True fracture strain, $Ln\ (A_i / A_f)$ (%)	0.5
True fracture stress, $\sigma_f = \frac{P_f}{A_f}$ (MPa)	933
Bridgman correction $= \frac{P_f}{A_f} \Big/ \left(1+\frac{4R}{D_f}\right) Ln\left(1+\frac{D_f}{4R}\right)$ (MPa)	836
Monotonic tensile strength coefficient, K (MPa)	N/A
Monotonic tensile strain hardening exponent, n	N/A
Hardness, Rockwell C (HRC)	57
Cyclic Properties	
Cyclic Yield Strength, (0.2% offset)$= K'(0.002)^{n'}$ (MPa)	N/A
Cyclic strength coefficient, K' (MPa)	N/A
Cyclic strain hardening exponent, n'	N/A
Fatigue Strength Coefficient, σ'_f (MPa)	9959
Fatigue Strength Exponent, b	-0.252
Fatigue Ductility Coefficient, ε'_f	N/A
Fatigue Ductility Exponent, c	N/A
Cyclic Elastic Modulus, E_c (MPa)	204,860

P_f: Load at fracture.
A_i and A_f: Specimen cross-section area before and after fracture.
R: Specimen neck radius.
D_f Specimen diameter at fracture

Appendix 1

SEM test results from Daimler Chrysler

Test Results

SEM Analysis/Fractography - 126898

Fracture Analysis (Performed By: Gerry Shulke)

One half of the fracture was cleaned with acetone and examined using Scanning Electron Microscopy (SEM). The fracture origin was intergranular. The fracture slowly transitioned into more and more microvoids as you progress across the fracture surface. The entire outer perimeter contained a shear lip, except at the fracture origin. There were no obvious signs of fatigue.

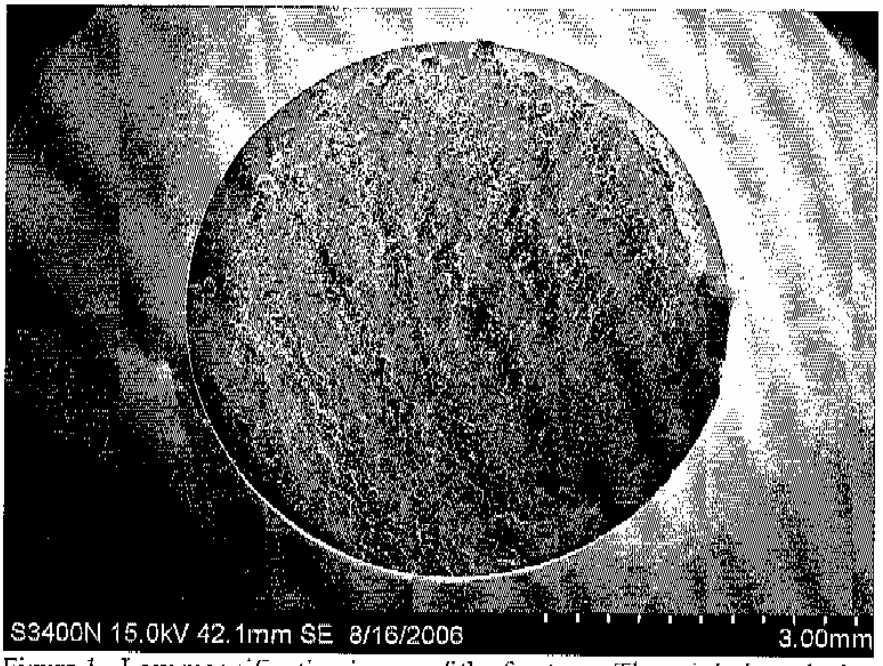

Figure 1. Low magnification image of the fracture. The origin is at the bottom o fthe image.

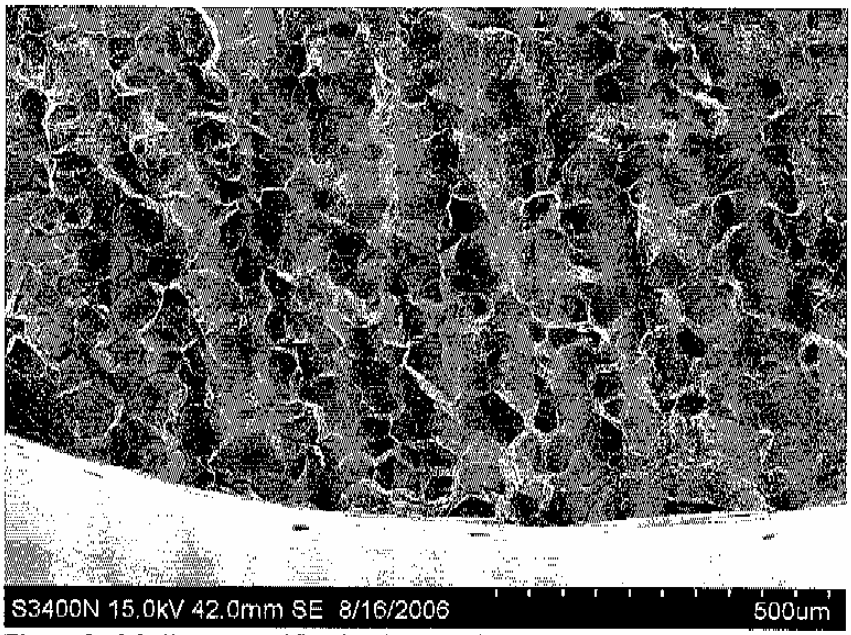

Figure 2. Medium magnification image of the origin area, which contained intergranular facets.

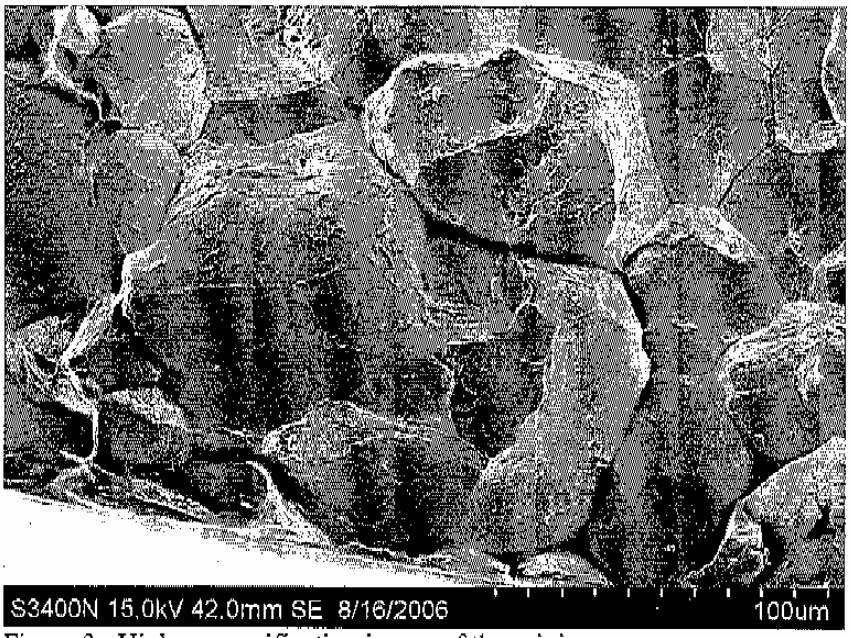

Figure 3. Higher magnification image of the origin area.

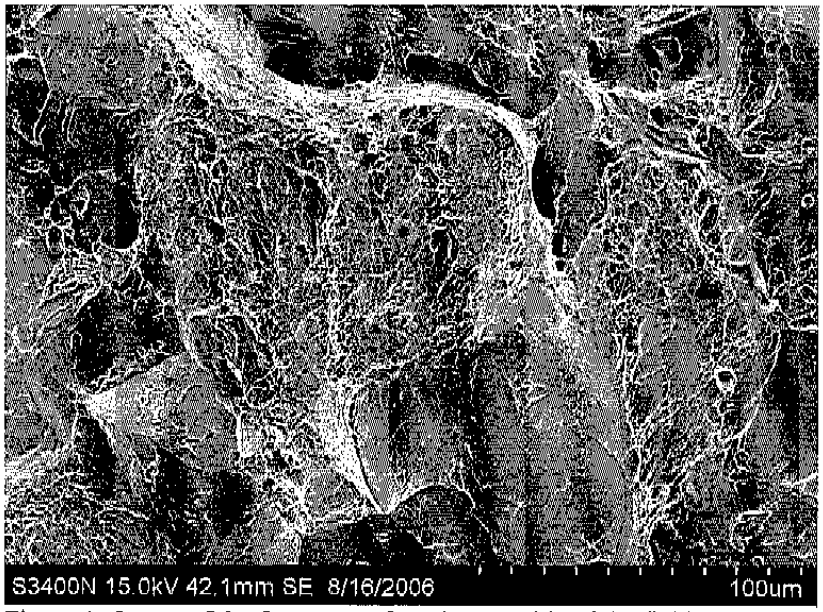

Figure 4. Image of the fracture surface, just outside of the field of view in figure 2. The fracture is a mixture of intergranular facets and collections of microvoids.

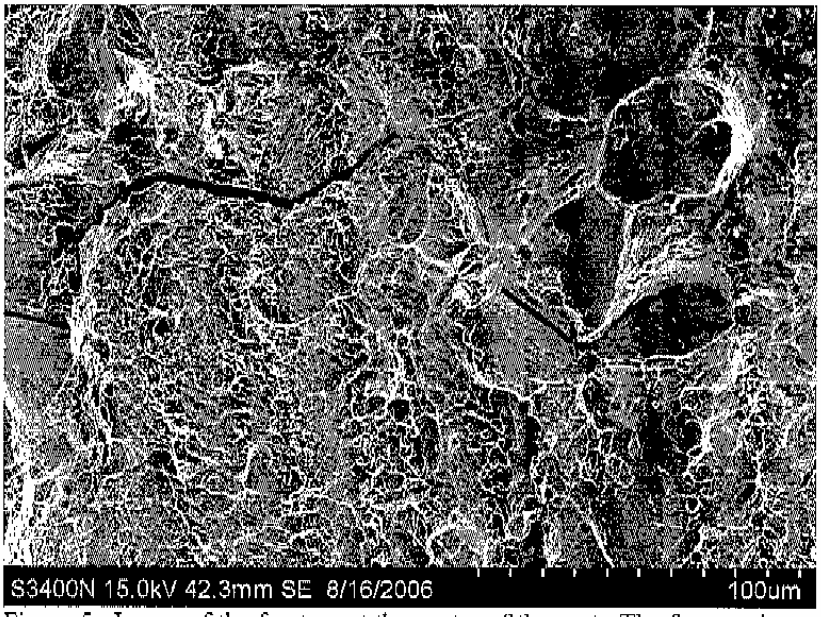

Figure 5. Image of the fracture at the center of the part. The fracture is predominately microvoids with some intergranular facets.

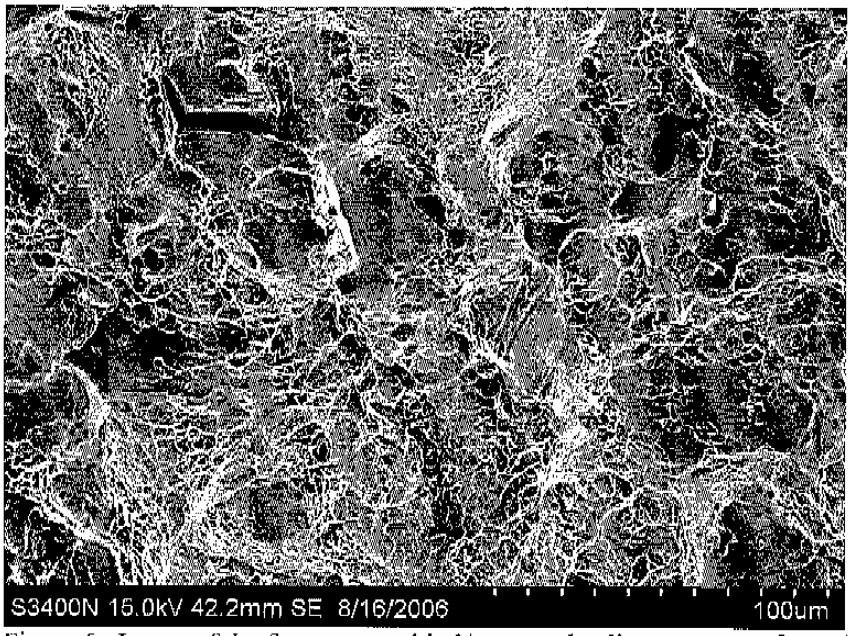

Figure 6. Image of the fracture roughly ¾ across the diameter away from the origin. The fracture is predominately microvoids, with a few intergranular facets.

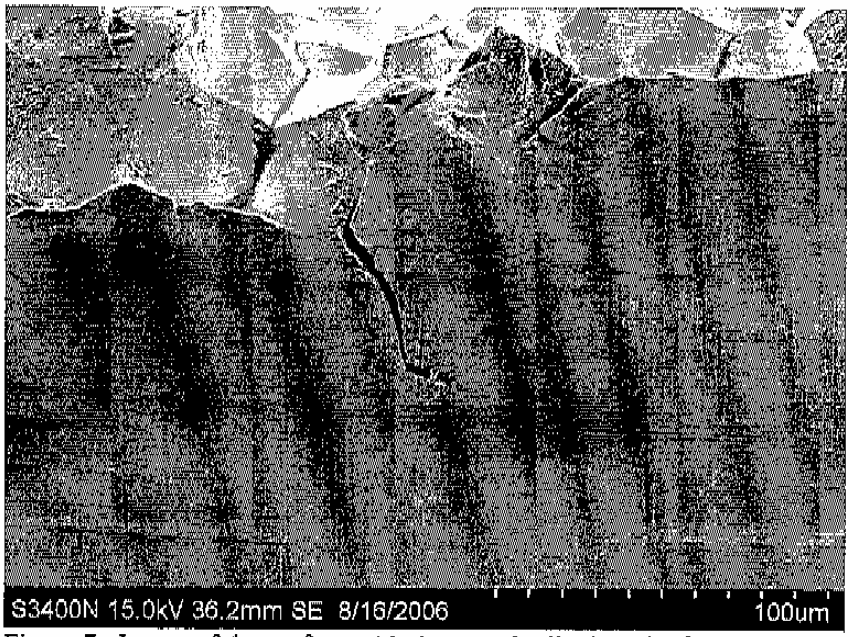

Figure 7. Image of the surface with the sample tilted, at the fracture origin.